Donor levels and the microscopic structure of the *DX* center in *n*-type Si-doped $Al_xGa_{0.51-x}In_{0.49}P$ grown by molecular-beam epitaxy

J. Mäkinen, T. Laine, J. Partanen, K. Saarinen, and P. Hautojärvi
Laboratory of Physics, Helsinki University of Technology, 02150 Espoo, Finland

K. Tappura, T. Hakkarainen,* H. Asonen, and M. Pessa
Department of Physics, Tampere University of Technology, P.O. Box 692, 33101 Tampere, Finland

J. P. Kauppinen, K. Vänttinen, and M. A. Paalanen
Department of Physics, University of Jyväskylä, P.O. Box 35, 40351 Jyväskylä, Finland

J. Likonen
Chemical Technology, Technical Research Center of Finland, P.O. Box 1404, 02044 VTT, Finland

(Received 25 May 1995; revised manuscript received 31 October 1995)

We have investigated donor levels and the local structure of *DX* centers in Si-doped $Al_xGa_{0.51-x}In_{0.49}P$ grown by gas-source molecular-beam epitaxy. In a ternary alloy $Ga_{0.51}In_{0.49}P$, Si donors form only shallow donor states. In contrast, in quaternary alloys with $x \geqslant 0.25$ a deep electron trapping center is observed. Hall measurements reveal an activated behavior of the mobile electron concentration, and the thermal binding energy of the dominant donor state is ~ 0.1 eV when the Al fraction is $x = 0.25$. Illumination with infrared or red light results in persistent photoconductivity at $T \leqslant 120$ K. The appearance of the *DX* level in the band gap around $x \approx 0.1$ gives a consistent picture of the experimental findings. Positron annihilation spectroscopy shows that the Si *DX* center is a vacancylike defect with a local structure equivalent to that found earlier in $Al_xGa_{1-x}As$. The very different core shell structures of the group-III (Ga, In) and group-V (P) atoms give direct evidence that the vacancy has P atoms as its nearest neighbors and we identify it as a vacancy in the group-III sublattice. The structural data give support to the vacancy-interstitial model, which predicts that the donor impurities can take two different configurations in *sp*-bonded semiconductors.

I. INTRODUCTION

Quaternary (Al,Ga,In)P semiconductor alloys have recently received a lot of interest as materials for visible optoelectronic devices. $Al_xGa_{0.51-x}In_{0.49}P$ alloys provide the largest direct band gap of all III-V semiconductor systems which can be grown lattice matched to GaAs. High-power laser diodes based on these materials have been demonstrated in the visible region at 630–700-nm wavelengths.[1,2]

It has become clear that group-IV and -VI donors have unusual properties in many *n*-type III-V alloys and compounds.[3,4] Besides the ordinary effective-mass states, relatively deep (thermal ionization energy ~ 0.1 eV) electron levels are observed, and there is strong evidence that they correspond to isolated donor impurities. This center is designated as a *DX* center.[5,6] The occupation of the *DX* level reduces the number of electrons in the conduction band, and limits the conductivity of an *n*-type material. It also causes some serious problems in field-effect transistors fabricated with *n*-type $Al_xGa_{1-x}As$ as electron trapping at the *DX* center results, e.g., in persistent or transient shifts of the threshold voltage.[7–9]

In the $Al_xGa_{1-x}As$ system in which the DX center has been most thoroughly investigated, a deep level appears in the band gap when the conduction-band edge is shifted upwards either due to Al alloying or application of hydrostatic pressure.[3,4] There is no simple way to predict for which impurity atoms and host crystals the metastable states are relevant. It appears, however, that the position of the conduction-band minimum is an important factor in determining whether the deep electron level is in the band gap. In $Al_xGa_{0.51-x}In_{0.49}P$ the direct band gap increases from 1.9 eV in the ternary alloy $Ga_{0.5}In_{0.49}P$ to approximately 2.3 eV at the crossover from the direct to indirect band gap at $x \approx 0.33$.[10] From this point of view it is not surprising that the formation of *DX*-like centers has been observed in *n*-type $Al_xGa_{0.51-x}In_{0.49}P$ when $x > 0.1$.[11,12]

The *DX* center has some very unusual properties not expected from an effective-mass donor. They include a large energy barrier for the capture of an electron, resulting in nonequilibrium occupation of electron levels at low temperatures. Optical ionization of the *DX* center leads to the persistent photoconductivity with electrons remaining in the conduction band, or to the capture of electrons at the shallow donor states. Further, the optical ionization energy of the *DX* center (~ 1 eV) is much larger than its thermal ionization energy. These properties have been advanced as an indication of the dominant role of lattice relaxation effects on the electron capture and emission.[3,4,6] The same conclusion was reached by Chadi and Chang[13] from self-consistent pseudopotential total-energy calculations. They find that donors can exist in two different configurations. One is the simple substitutional donor which gives rise to the effective-mass states. The other is characterized by a large displace-

0163-1829/96/53(12)/7851(12)/$10.00 © 1996 The American Physical Society

ment of the column-IV donor atom along the ⟨111⟩ direction. To take Si as an example, the distorted geometry can be viewed as a vacancy-Si-interstitial pair at a threefold-coordinated site. This state is highly localized and negatively charged. The bonding is largely sp^2 like, and it was suggested that the metastability of point defects is an intrinsic property of sp-bonded semiconductors.[13,14]

It has become increasingly evident that the vacancy-interstitial model accounts for the electrical and optical properties of the *DX* center. The same basic mechanism has been used to explain the metastability of the *EL*2 center in GaAs.[15,16] The existence of *DX*-like centers was also predicted in some II-VI compounds.[17] Although evidence of the generality of metastable states associated with impurities which normally give rise to effective-mass states has accumulated, there is very little direct structural data about the *DX* center to finally confirm its origin.

The aim of this paper is to study the effects of alloy composition and doping on the states of the Si donors in $Al_xGa_{0.51-x}In_{0.49}P$ grown by gas-source molecular-beam epitaxy. A particular aim is to broaden the scope of the previous studies of the *DX* center[18,19] to obtain further information about its local structure. For that purpose we have combined photo-Hall measurements, secondary-ion-mass spectrometry (SIMS), and positron annihilation experiments.

The findings of this work can be summarized as follows. In the ternary alloy $Ga_{0.51}In_{0.49}P$ the free-electron concentration follows the number of Si dopants up to a very high donor concentration of 3×10^{19} cm^{-3}. In quaternary alloys with $x\geqslant0.25$ the maximum free-electron concentration attained was approximately 10^{18} cm^{-3}. Hall measurements reveal a large thermal ionization energy of the donors (50–100 meV). Persistent photoconductivity is observed at low temperatures. These properties lead us to conclude that Si atoms form *DX* centers in n-type $Al_xGa_{0.51-x}In_{0.49}P$. The local structure of the *DX* center determined by positron annihilation spectroscopy is equivalent to that found earlier in $Al_xGa_{1-x}As$. In particular, we find that when the deep level is filled, the Si-*DX* center is a vacancylike defect. The different core shell structures of the group-III (Ga, In) and -V (P) atoms suggest a direct identification of the vacancy. We find clear evidence that the vacancy is in the group-III sublattice. These structural data give support to the theoretical vacancy-interstitial model.[13,14]

II. EXPERIMENTAL DETAILS

A. Layers grown by gas-source molecular-beam epitaxy

$Al_xGa_{0.51-x}In_{0.49}$ P quaternary ($x\approx0.25$ and 0.36) and ternary ($x=0$ and 0.51) alloys were grown lattice matched on GaAs(001) substrates by gas-source molecular-beam epitaxy (GSMBE). The GSMBE chamber is a part of a dual reactor chamber V80H built by VG Semicon. In this system[20] group-V materials (As_2 and P_2) were obtained by a thermal decomposing of the corresponding hydride gases in a high-pressure cracking cell at 950°C, while the group-III (Al, Ga, and In) and dopant material (Si and Be) beams were generated from conventional solid source effusion cells. A calibrated ion gauge was used to determine the Ga and In fluxes. The group-V beams were controlled by adjusting the hydride pressures in the high-pressure regions of the gas sources. The substrates (16×16 mm^2 in size) were attached to the sample holder without indium solder, and were heated by direct thermal radiation. A narrow-band infrared pyrometer was used to measure the substrate temperature. Pregrowth heat treatment of the substrates was performed under As_2 pressure at 600–610°C. The substrate temperature was kept near 520–525°C during the growth of the $Ga_{0.51}In_{0.49}P$ and the quaternary layers, while the $A_{0.51}In_{0.49}P$ films were grown near 490°C.

A series of both 1- and 2-μm-thick layers were grown with different Si and Be doping concentrations, and also without intentional doping. The nominal Si concentrations from 8×10^{17} to 3×10^{19} cm^{-3} were obtained by adjusting the Si cell temperature T_{Si} according to the carrier concentration-vs-T_{Si} data calibrated for GaAs, in which practically all Si atoms are known to be active at the concentrations used. The lattice constants were determined by measuring x-ray-diffraction rocking curves with a Bede Scientific Instruments Model 150 diffractometer using Cu *Kα* radiation and (004) reflection.

B. Experimental techniques

SIMS analyses were made using a double-focusing magnetic sector spectrometer (VG Ionex IX70S).[21] The samples were bombarded with 10-keV Cs^+ ions at a 21° angle of incidence. The ion current was typically 50 nA during the depth profiling, and the primary ion beam was raster scanned over an area of 340×370 μm^2. Crater wall effects were avoided by using a 10% electronic gate. The pressure inside the analysis chamber was typically 10^{-7} Pa during the measurements. The Si concentration was determined by using ion-implanted reference samples. 80-keV ^{28}Si ions, the total fluence of which was 1×10^{15} cm^{-2}, were implanted into $Al_xGa_{0.51-x}In_{0.49}P$ layers with $x=0$, 0.36, and 0.51. The SIMS instrument was calibrated by extracting the relative sensitivity factor (RSF) from the analyses of the reference samples.[22]

The Hall measurements were conducted in a commercial He cryostat from Oxford Instruments. The cryostat had a variable temperature insert inside a 10-T superconducting magnet. The insert had a top-loading capability, and its temperature range could be extended from 4 K all the way to 320 K.

The longitudinal resistance ρ_{xx} and the Hall resistance ρ_{xy} were measured with a sensitive lock-in technique using a low excitation current of a few microamperes at 70-Hz frequency. The classical Hall resistance of a thin sample with a thickness t at a magnetic field B can be expressed by the formula $\rho_{xy}=-B/etn_{\mathrm{Hall}}$, where n_{Hall} is the three-dimensional density of mobile carriers. From the linear ρ_{xy}-vs-B plots one can first determine the Hall coefficient $R_{\mathrm{Hall}}=\rho_{xy}/B$ and then the carrier density $n_{\mathrm{Hall}}=-1/eR_{\mathrm{Hall}}$.

Positron annihilation[23,24] in the epitaxial layers was investigated using the low-energy positron beam technique.[25] The 511-keV annihilation line was recorded with a high-purity Ge detector, and typically 5×10^6 counts were collected to the annihilation peak. The sample temperature was controlled between 20 and 300 K with a closed-cycle He cryocooler and a resistive heater, and measured with a silicon

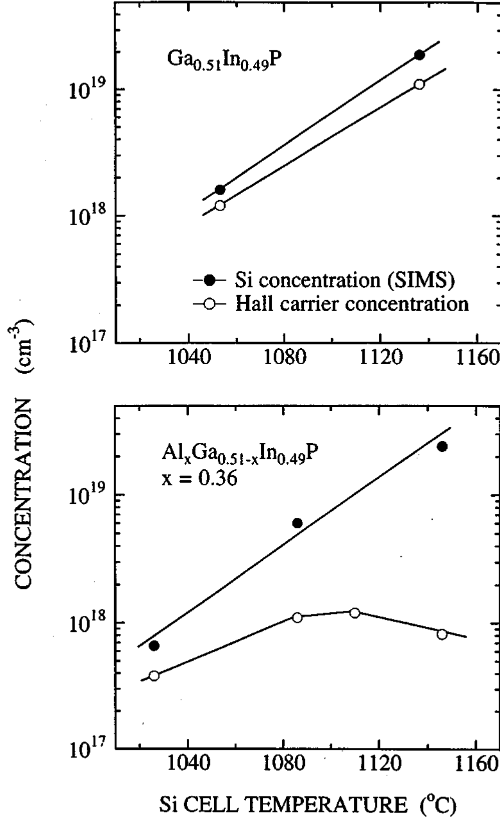

FIG. 1. Si and Hall carrier concentrations at $T=295$ K vs the Si cell temperature in a ternary alloy $Ga_{0.51}In_{0.49}P$ (samples 1 and 2) and in a quaternary alloy $Al_xGa_{0.51-x}In_{0.49}P$ with $x=0.36$ (samples 4–7). Si concentrations were measured using secondary-ion-mass spectrometry. The solid lines are guides to the eye.

diode temperature sensor. Above room temperature the sample was heated with an electron-beam heater, and its temperature was measured with a type-K thermocouple mounted to the sample surface. A GaAs infrared (IR) light-emitting diode was used for illumination (photon energy ~ 1.3 eV). The light intensity measured with a Ge photodetector was typically 0.1 mW/cm^2.

Observation of positron trapping at a vacancy defect is based on the Doppler broadening of the annihilation radiation.[23] The shape of the 511-keV annihilation line, convoluted with the resolution of the Ge detector, can be described in terms of valence and core electron annihilation. The low-momentum part is characterized by the valence annihilation parameter S, which is defined as the number of annihilation events over the energy range 511 keV $\pm \Delta E \gamma$ ($\Delta E_\gamma = 0.95$ keV) around the centroid of the peak. It represents the fraction of electron-positron pairs with a longitudinal momentum component $p_L \leqslant 0.5$ a.u. ($p_L/m_0 c \leqslant 3.7\times 10^{-3}$, where m_0 is the electron mass). The core annihilation parameter W is calculated from the tail of the peak, 2.9 keV $\leqslant |\Delta E \gamma| \leqslant 7.3$ keV. As defined here, it corresponds to annihilations with a large momentum component p_L between 1.6 and 3.9 a.u. (or $11\times 10^{-3} \leqslant p_L/m_0 c \leqslant 28\times 10^{-3}$), which are almost totally due to the core electrons.

Besides the conventional single-detector Doppler measurements, we used the coincidence measurement of both 511-keV annihilation gamma rays to reduce the background.[26–28] With this technique the momentum distribution can be studied up to much higher momentum values.

III. EXPERIMENTAL RESULTS

A. Si doping of $Al_xGa_{0.51-x}In_{0.49}P$

Si-atom concentrations in the GSMBE-grown layers were obtained by adjusting the Si cell temperature between 950 and 1150°C. The Si concentration determined by SIMS and the Hall carrier concentration at 295 K are plotted against the Si cell temperature in Fig. 1 for the ternary alloy $Ga_{0.51}In_{0.49}P$ and the quaternary alloy $Al_xGa_{0.51-x}In_{0.49}P$ with $x=0.36$. The results of the SIMS and the Hall measurements at room temperature are also summarized in Table I.

The number of Si atoms incorporated into the material follows the increase of the Si vapor pressure in both samples. The number of free electrons in the conduction band, however, depends strongly on the alloy composition. In $Ga_{0.51}In_{0.49}P$, the Hall carrier concentration increases with the Si cell temperature in proportion to the Si concentration. Even at a very high Si concentration, 2.1×10^{19} cm^{-3}, Si atoms are electrically activated as shallow donors and compensation remains relatively small, as indicated by the Hall carrier concentration 1.2×10^{19} cm^{-3}.

In $Al_xGa_{0.51-x}In_{0.49}P$ with $x=0.36$, the Hall carrier concentration does not increase above $(1–2)\times 10^{18}$ cm^{-3}, independent of the number of Si atoms. When the concentration of Si atoms is 5×10^{18} cm^{-3}, the concentration of electrons in the conduction band is less than 20% of the total number of Si atoms, and it collapses to $\sim 3\%$ at the highest doping level 2.6×10^{19} cm^{-3}. The Hall carrier concentration is also clearly smaller than the Si concentration in the layer in

TABLE I. Al fractions x, nominal doping levels, experimental Si concentrations from SIMS analyses, the Hall carrier concentrations at 295 K, and the activation energies E_a of the mobile electron concentration in Si-doped $Al_xGa_{0.51-x}In_{0.49}P$ layers. The layers were grown by gas-source molecular-beam epitaxy (GSMBE), and lattice matched to GaAs.

Sample	x	Doping (cm^{-3})	SIMS concentration (cm^{-3})	n_{Hall} (295 K) (cm^{-3})	E_a (meV)
1-μm layers					
1	0	8×10^{17}	1.6×10^{18}	1.2×10^{18}	0
2	0	1×10^{19}	2.1×10^{19}	1.1×10^{19}	
3	0.25	8×10^{17}		1.7×10^{17}	98
4	0.36	8×10^{17}	7.2×10^{17}	3.8×10^{17}	79
5	0.36	5×10^{18}	6.6×10^{18}	1.1×10^{18}	
6	0.36	$\times 10^{19}$		1.2×10^{18}	
7	0.36	3×10^{19}	2.6×10^{19}	8.2×10^{17}	
8	0.51	8×10^{17}	1.0×10^{18}	5.0×10^{17}	42
2-μm layers					
9	0	5×10^{18}		8.7×10^{18}	0
10	0.36	5×10^{18}		1.8×10^{18}	78
11	0.51	5×10^{18}		3.3×10^{18}	

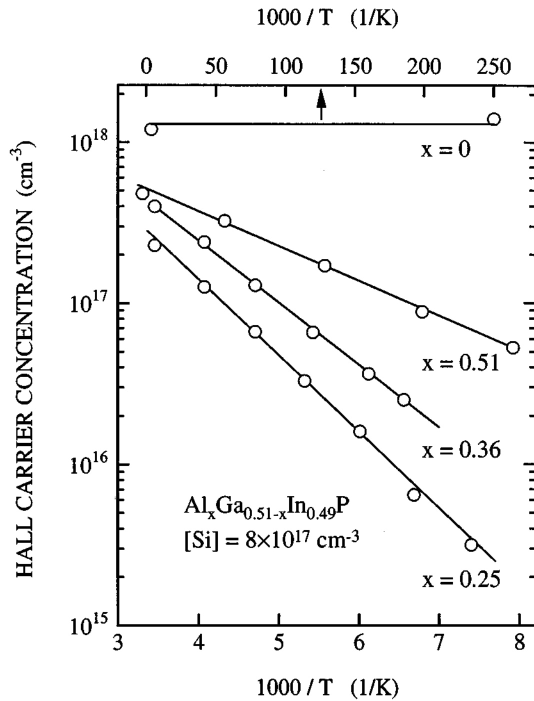

FIG. 2. Hall carrier concentrations $n_{\mathrm{Hall}}=-1/eR_{\mathrm{Hall}}$ determined from the Hall resistivity ρ_{xy} plotted as a function of the inverse temperature T^{-1}. The alloy composition varies from $x=0$ ($Ga_{0.51}In_{0.49}P$) to $x=0.51$ ($Al_{0.51}In_{0.49}P$), and the nominal Si concentration in all layers is 8×10^{17} cm^{-3} (samples 1, 3, 4, and 8). The thermal activation energies of the mobile electron concentration are given in Table I. The solid lines are fits to the data.

which $x=0.25$ and in the ternary alloy $Al_{0.51}In_{0.49}P$ ($x=0.51$) when the nominal doping level is 8×10^{17} cm^{-3} (Table I).

The temperature dependence of the concentration of the mobile electrons, to be discussed in more detail in Sec. III B, gives further insight into the properties of the Si donors. In $Al_xGa_{0.51-x}In_{0.49}P$ with $x=0.25$, the Hall carrier concentration decreases almost by two orders of magnitude from 295 to 135 K (Fig. 2). This very rapid decrease of the free-electron concentration suggests the existence of a deep electron trapping center. In contrast, the Hall carrier concentration in the ternary alloy $Ga_{0.51}In_{0.49}P$ is almost independent of temperature all the way down to 4 K. The formation of a deep electron trapping center in Si-doped $Al_xGa_{0.51-x}In_{0.49}P$, in which $x=0.24$ at a concentration far exceeding the concentration of the shallow states was earlier reported by Nojima, Tanaka, and Asahi.[11] The difference between the doping concentration [Si] and the carrier concentration n_{Hall} becomes larger when [Si] increases (Fig. 1), suggesting that the concentration of the deep electron trap increases with the Si concentration.

In conclusion, we can suppose that a deep electron trapping center related to Si doping is formed in $Al_xGa_{0.51-x}In_{0.49}P$. It suggests that the difference between $Ga_{0.51}In_{0.49}P$ and $Al_xGa_{0.51-x}In_{0.49}P$ illustrated in Fig. 1 is due to the different states of the Si donors.

B. Analysis of the Hall measurements

1. Temperature dependence of the Hall carrier concentration

The Hall carrier concentrations n_{Hall} calculated using the simple relation $n_{\mathrm{Hall}}=-1/eR_{\mathrm{Hall}}$ are plotted against the reciprocal temperature T^{-1} in Fig. 2 between 300 and 100 K. In all layers the nominal Si concentration is 8×10^{17} cm^{-3}, and the Si concentrations determined by SIMS are given in Table I. Figure 2 illustrates the difference between the ternary alloy $Ga_{0.51}In_{0.49}P$ and quaternary alloys with $x\geq0.25$. In n-type Si-doped $Ga_{0.51}In_{0.49}P$, the mobile electron concentration decreases less than a factor of 2 from 300 to 4 K. In quaternary $Al_xGa_{0.51-x}In_{0.49}P$ ($x=0.25$ and 0.36) as well as in $Al_{0.51}In_{0.49}P$ the Hall carrier concentration is strongly temperature dependent, indicating the trapping of free electrons by deep centers.

The linear $\ln(n_{\mathrm{Hall}})-T^{-1}$ dependence over a decade in the Hall carrier concentration from 300 to 120 K clearly demonstrates an activated behavior of the electron density. The activation energies E_a calculated from the slopes of the $\ln(n_{\mathrm{Hall}})$-vs-T^{-1} curves are given in Table I and they depend strongly on the alloy composition. Comparison of $Ga_{0.51}In_{0.49}P$ and $Al_xGa_{0.51-x}In_{0.49}P$ ($x=0.25$), which both have a direct band gap, demonstrates the deepening of the donor level. In $Ga_{0.51}In_{0.49}P$, in which the compensation is negligible, the thermal activation energy is zero. The Si concentration is probably sufficiently high for the insulator-to-metal transition to occur. When the Al concentration increases, the deep states appear with a maximum activation energy $E_a\approx0.1$ eV around $x=0.25$. For the shallow donor states related to the Γ minimum of the conduction band a similar activation energy as in $Ga_{0.51}In_{0.49}P$ is expected ($\sim$2 meV according to Ref. 29). At higher Al concentrations the activation energy decreases to 79 meV at $x=0.36$ and 42 meV in $Al_{0.51}In_{0.49}P$.

2. Persistent photoconductivity

To illustrate the persistent photoconductivity effect, the Hall carrier concentration n_{Hall} and the longitudinal resistance ρ_{xx} measured in $Al_xGa_{0.51-x}In_{0.49}P$ ($x=0.36$) are plotted in Fig. 3(a). n_{Hall} was measured after cooling the samples in the dark from 300 K, and after illumination with 940-nm IR light at 74 K. ρ_{xx} was measured after cooling the samples in the dark and after illumination at each temperature. Figure 3(b) shows the longitudinal resistance ρ_{xx} in $Al_{0.51}In_{0.49}P$. This layer was illuminated with red light. The nominal Si concentration of both samples is 5×10^{18} cm^{-3}.

In Si-doped $Al_xGa_{0.51-x}In_{0.49}P$ a freeze-out of electrons into a deep electron level is observed when the temperature is lowered from 300 to 120 K. The slope of the Arrhenius plot yields the activation energy $E_a=78$ meV. It is equal to the activation energy in the sample which has the same alloy composition ($x=0.36$) but a smaller Si concentration 8×10^{17} cm^{-3} (Table I). If the sample is exposed to IR light below 100 K, the concentration of the conduction electrons increases. The Hall carrier concentration 4×10^{17} cm^{-3} at 74 K after illumination is an order of magnitude larger than before illumination. This photoinduced increase of the electron concentration persists at low temperatures. Around 70 K a very slow decrease of the Hall carrier concentration with

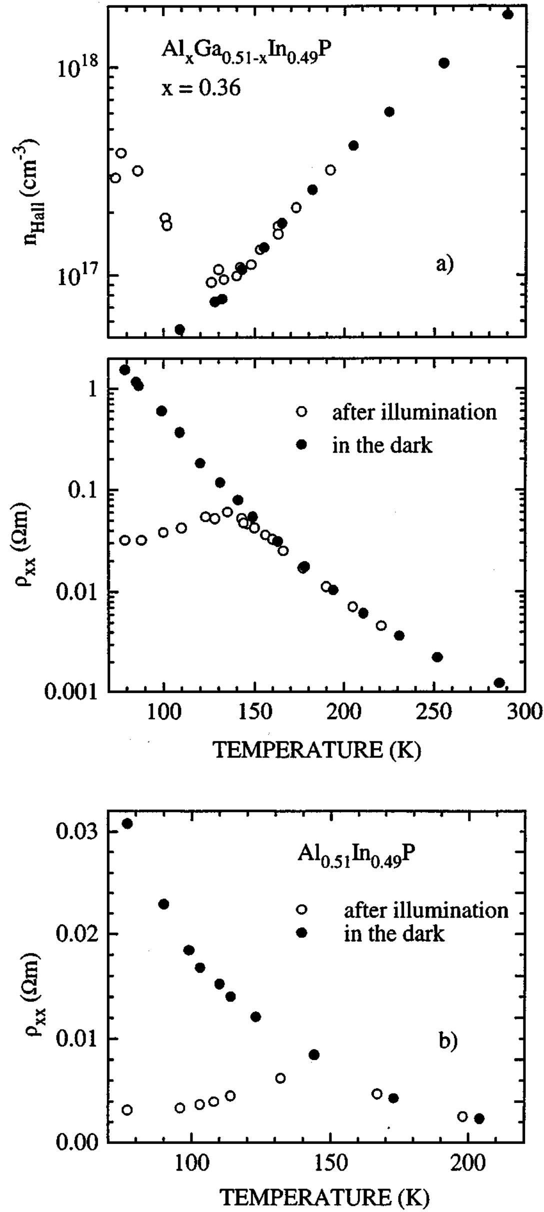

FIG. 3. (a) Hall carrier concentration n_{Hall} and the longitudinal resistance ρ_{xx} in $\mathrm{Al}_x\mathrm{Ga}_{0.51-x}\mathrm{In}_{0.49}\mathrm{P}$ with $x=0.36$, and a Si concentration of 5×10^{18} cm^{-3} (sample 10) measured after cooling the sample in the dark from 300 K, and after illumination with IR light at 74 K (n_{Hall}) or at each temperature (ρ_{xx}). (b) The longitudinal resistance ρ_{xx} in $\mathrm{Al}_{0.51}\mathrm{In}_{0.49}\mathrm{P}$ in which the Si concentration is 5×10^{18} cm^{-3} (sample 11). ρ_{xx} was measured after cooling the sample in the dark from 300 K, and after illumination with red light at 75 K.

time is seen. When temperature is raised further the photoconductivity finally disappears, and by 140 K the Hall carrier concentration n_{Hall} has recovered to its equilibrium value.

The longitudinal resistance ρ_{xx} also shows a persistent increase of the conductivity after illumination (Fig. 3). Below 200 K the resistivity in $\mathrm{Al}_x\mathrm{Ga}_{0.51-x}\mathrm{In}_{0.49}\mathrm{P}$ ($x=0.36$) in the dark increases much more rapidly than expected from the decrease of the Hall carrier concentration. It shows a strong increase of electron scattering at low temperatures. Illumination with IR light at 75 K decreases the resistivity by almost two orders of magnitude. This decrease is far larger than the increase of the concentration of mobile electrons, indicating that, besides the concentration of mobile electrons, the electron mobility is also higher after illumination. A persistent decrease of the resistance ρ_{xx} is seen also in $\mathrm{Al}_{0.51}\mathrm{In}_{0.49}\mathrm{P}$, which was illuminated with red light. In both samples the resistivity returns to its equilibrium value by 150 K. In Si-doped $\mathrm{Ga}_{0.51}\mathrm{In}_{0.49}\mathrm{P}$ layers in which the donor activation energy is zero and compensation is small, illumination has no influence on the free-electron concentration in the conduction band.

The Hall measurements demonstrate the well-known persistent photoconductivity effect which is observed in many n-type III-V compounds.[3] The Hall carrier concentration is very similar to that observed in $\mathrm{Al}_x\mathrm{Ga}_{1-x}\mathrm{As}$ in the range of the alloy composition in which the band gap is indirect.[30,31]

C. Positron annihilation

1. Vacancy-type defects in n-type $\mathbf{Al_xGa_{0.51-x}In_{0.49}P}$

Positron annihilation was measured in the undoped and Si-doped layers described in Table I. We first discuss the correlation between the alloy composition, Si doping, and the vacancy defects. In Sec. III C 2, the temperature dependence of positron annihilation is presented, and we will demonstrate the effect of illumination on the vacancy signal.

The core annihilation parameter varies with the alloy composition. This was observed earlier in $\mathrm{Al}_x\mathrm{Ga}_{1-x}\mathrm{As}$,[18] and it can be attributed to the smaller positron annihilation rate with core electrons when Ga is replaced by Al. To compare layers with different alloy compositions, the core annihilation parameters are normalized to free positron annihilation at the same alloy composition to give W/W_B. We take W_B as the value measured in an undoped layer or in a p-type Be-doped (8×10^{17} cm^{-3}) layer which yield identical core and valence annihilation parameters. The temperature dependence of the Doppler parameters also suggest that only free positron annihilation can be seen in the undoped layers (see Sec. III C 2).

The core annihilation parameters W/W_B (295 K) in Si-doped $\mathrm{Al}_x\mathrm{Ga}_{0.51-x}\mathrm{In}_{0.49}\mathrm{P}$ measured at room temperature are plotted against the nominal Si concentration in Fig. 4. The core annihilation parameters are systematically smaller in the Si-doped layers than in the undoped layers. The reduced core electron annihilation gives an indication of positron trapping at vacancy-type defects. We find a strong dependence of the core annihilation parameter both on the alloy composition and the Si concentration. In $\mathrm{Al}_x\mathrm{Ga}_{0.51-x}\mathrm{In}_{0.49}\mathrm{P}$ with $x\geqslant0.25$, positron trapping is already observed at the Si concentration 8×10^{17} cm^{-3}. In $\mathrm{Ga}_{0.51}\mathrm{In}_{0.49}\mathrm{P}$, positron trapping is first observed at a much higher Si concentration 5×10^{18} cm^{-3}. In the quaternary alloy $x=0.36$ the core annihilation parameter becomes independent of the doping when the doping level is 5×10^{18} cm^{-3} or higher. This gives an indication of the saturation of positron trapping, i.e., all positrons annihilate at vacancy defects. Below we will demonstrate that the defects which dominate positron trapping in $\mathrm{Al}_x\mathrm{Ga}_{0.51-x}\mathrm{In}_{0.49}\mathrm{P}$ ($x\geqslant0.25$) cannot be observed in $\mathrm{Ga}_{0.51}\mathrm{In}_{0.49}\mathrm{P}$.

The measured core annihilation parameters W can be used to calculate the positron trapping rates and to estimate the

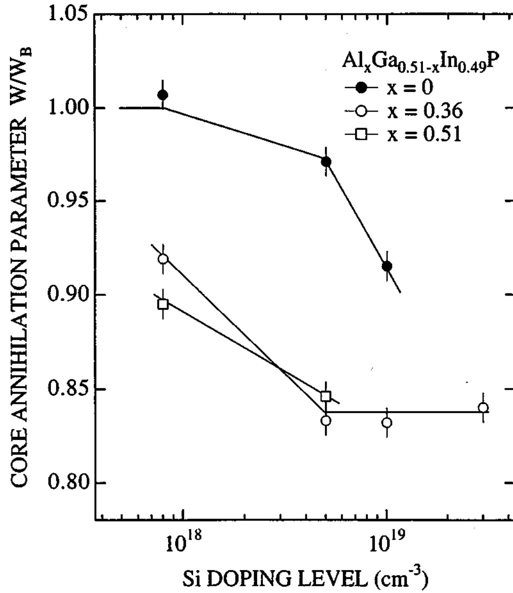

FIG. 4. Plot of the core annihilation parameter at $T=295$ K against the nominal Si concentration in $Ga_{0.51}In_{0.49}P$ (samples 1, 2, and 9), $Al_xGa_{0.51-x}In_{0.49}P$ with $x=0.36$ (samples 4–7), and $Al_{0.51}In_{0.49}P$ (samples 8 and 11). To compare samples with different Al concentrations, the core annihilation parameters are normalized to the core annihilation parameter for free positron annihilation W_B at the same alloy composition to give W/W_B (295 K). The solid lines are guides to the eye.

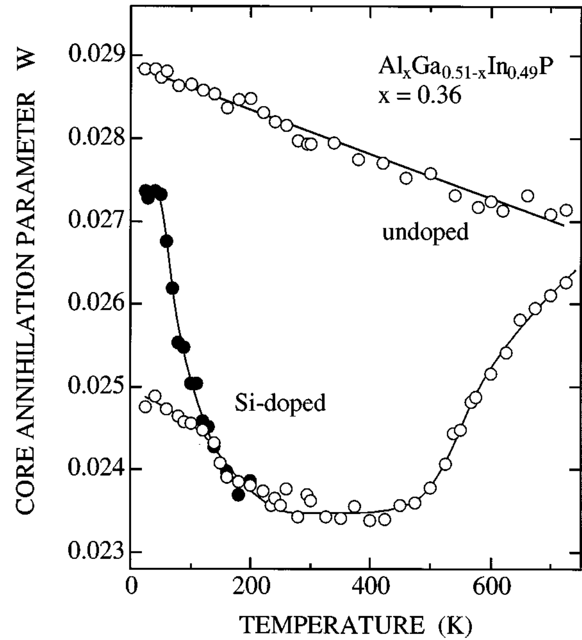

FIG. 5. The temperature dependence of the core annihilation parameter in undoped and Si-doped $Al_xGa_{0.51-x}In_{0.49}P$ with $x=0.36$, and the Si concentration of 5×10^{18} cm^{-3} (sample 10). In the Si-doped layer the core annihilation was measured in the dark and after illumination with IR light at 20 K (all measurements are done in the dark). The solid lines are guides to the eye.

defect concentrations. Assuming that one defect dominates positron annihilation, the kinetic two-state trapping model[32] gives the fraction of positrons annihilating from the defect state as

$$f_D=\frac{\kappa}{\kappa+\lambda_B}=\frac{W_B-W}{W_B-W_D}. \quad (1)$$

In Eq. (1), the positron trapping coefficient μ (trapping rate per unit concentration of vacancies) and the vacancy concentration (C_V) give the positron trapping rate $\kappa=\mu C_V$, λ_B denotes the annihilation rate of free positrons, and W_D is the core annihilation parameter for positron annihilation at the defect state. When positron trapping is in saturation, all positrons annihilate at defects: $W=W_D$ and $f_D=1$.

In $Al_xGa_{0.51-x}In_{0.49}P$ with $x=0.36$, the core annihilation parameter in the layers in which the Si concentration is high (layers 5–7 and 10) gives $W_D/W_B=0.835(5)$ at 295 K. From Eq. (1), the positron trapping rate is $\kappa\approx\lambda_B$ in the layer with [Si] $=8\times10^{17}$ cm^{-3} (layer 4) in which trapping is not in saturation. The free positron annihilation rate in $Al_xGa_{0.51-x}In_{0.49}P$ is not known. However, the experimental bulk lifetimes 223 ps in GaP (Ref. 33) and 244 ps in InP (Ref. 28) indicate that to estimate the defect concentration we can take $\lambda_B=(1/244$ ps). Assuming the positron trapping coefficient $\mu=2\times10^{15}$ s^{-1},[34–37] the positron trapping rate would imply the vacancy concentration $C_V\approx1\times10^{17}$ cm^{-3}. For saturation trapping to occur, the positron trapping rate must be $\kappa>10\lambda_B$. This indicates that the vacancy concentration is higher than $C_V>1\times10^{18}$ cm^{-3} when the Si concentration is 5×10^{18} cm^{-3}.

The ternary alloy $Ga_{0.51}In_{0.49}P$ (layers 1, 2, and 9) shows no indication of a saturation of positron trapping, and therefore the defect parameter W_D is not known. We can, however, estimate the trapping rate $\kappa<0.3\lambda_B$ in layer 9, in which the Si concentration is 5×10^{18} cm^{-3} if we assume that the core annihilation parameter in layer 2 with the highest Si concentration 1×10^{19} cm^{-3} equals W_D. This would mean saturation positron trapping in that layer, and is bound to give an overestimate for the trapping rates. This shows that the positron trapping rate in $Ga_{0.51}In_{0.49}P$ is far smaller than in the $Al_xGa_{0.51-x}In_{0.49}P$ layer $x=0.36$ ($\kappa>10\lambda_B$) at the same doping level. As the positron trapping coefficients at room temperature for neutral and negatively charged vacancies in different semiconductors have been found to be rather similar, we conclude that the vacancy concentration is much smaller.

The appearance of the vacancy defects shows a correlation to the compensation of electrons which was demonstrated in Fig. 1. In $Ga_{0.51}In_{0.49}P$ the compensation ratio is small and the vacancy concentrations are small compared to the Si concentrations. In contrast to the ternary alloy ($x=0$), the vacancy concentration in n-type $Al_xGa_{0.51-x}In_{0.49}P$ samples is comparable to the number of Si atoms in the layer.

2. *Temperature dependence of positron annihilation and photoeffects*

The core annihilation parameters in undoped and Si-doped (5×10^{18} cm^{-3}) $Al_xGa_{0.51-x}In_{0.49}P$ with $x=0.36$ are plotted against temperature in Fig. 5. Positron annihilation was measured from 20 to 720 K, keeping the sample in the

dark throughout the measurement. The effect of illumination on positron annihilation was studied by measuring the core annihilation parameter in the dark as a function of temperature subsequent to the illumination of the sample with IR light at 20 K.

In the undoped layer, the increase of temperature causes a small and nearly linear decrease of the core annihilation parameter. Measurement of the core annihilation parameter in the undoped $Ga_{0.51}In_{0.49}P$ and $Al_{0.51}In_{0.49}P$ samples gives an equivalent temperature dependence. This can be attributed to the thermal lattice expansion,[38] and is commonly observed for free positron annihilation in solids.

In the Si-doped layer the core annihilation parameter between 300 and 20 K indicates positron trapping at vacancy defects. The small increase of the core annihilation parameter below 200 K in the dark indicates competitive trapping at some other defects. A possible cause is positron trapping at negatively charged ion-type centers at low temperatures. Such centers are commonly observed, e.g., in GaAs.[39–41] The two most singular features of Fig. 5 are an increase of the core annihilation parameter from 450 to 720 K, and its persistent increase at 20 K after exposure to IR light. The increase of the core annihilation parameter close to the values measured in the undoped layer at 700 K indicates that the vacancy which dominates positron annihilation below 400 K cannot be observed at high temperatures. The temperature variation of the core annihilation parameter from 400 to 700 K is totally reversible, and the disappearance of the vacancy signal is not due to annealing of defects in the layer.

Illumination with IR light at 20 K causes a persistent increase of the core annihilation parameter, i.e., a persistent disappearance of the vacancy signal. The photoeffect lasts at least several days, and we cannot observe the vacancy signal without warming the sample. The vacancy signal recovers above 60 K, and by 140 K the core annihilation parameter is equal to the value measured before illumination. In Si-doped $Al_{0.51}In_{0.49}P$ the temperature dependence of the core annihilation parameter is totally equivalent to that shown in Fig. 5. In particular, IR light causes a similar persistent increase of the core annihilation parameter at 20 K.

The vacancy signal cannot be totally removed by IR light in Si-doped $Al_xGa_{0.51-x}In_{0.49}P$ or $Al_{0.51}In_{0.49}P$. This indicates a residual concentration of vacancy-type defects which are insensitive to illumination. The concentration of those residual vacancies appears to be similar to the vacancy concentration in a Si-doped ternary alloy $Ga_{0.51}In_{0.49}P$. In $Ga_{0.51}In_{0.49}P$, illumination has no influence on positron annihilation.

Further insight into the metastable behavior of the vacancy was obtained through annealing experiments. The Si-doped $Al_xGa_{0.51-x}In_{0.49}P$ ($x=0.36$) and $Al_{0.51}In_{0.49}P$ layers were first cooled in the dark, and illuminated with IR light at 20 K. Positron annihilation was measured as a function of an isochronal annealing between 20 and 150 K in the dark. The core annihilation parameters are plotted against the annealing temperature in Fig. 6. The core annihilation parameter is constant from 20 K to approximately 50 K, whereafter the vacancy signal recovers in a rather broad temperature range, and by 120 K it is at the level measured before illumination indicating that the recovery is complete.

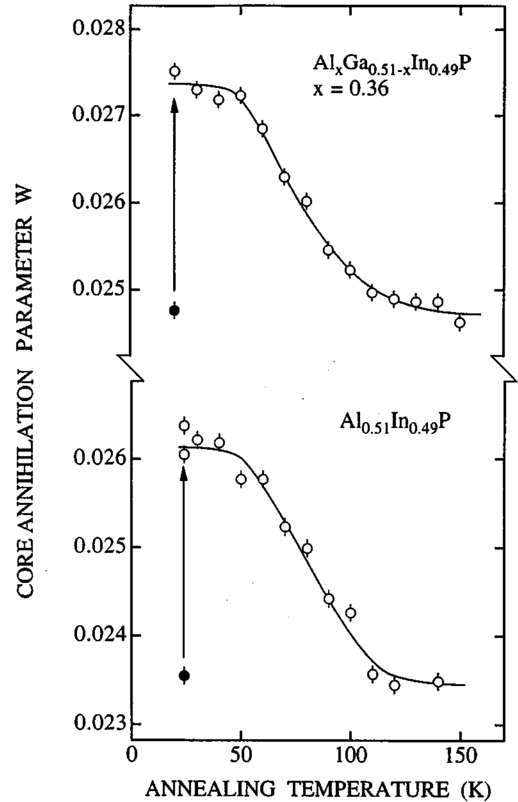

FIG. 6. The core annihilation parameter in $Al_xGa_{0.51-x}In_{0.49}P$ with $x=0.36$, and in $Al_{0.51}In_{0.49}P$ as a function of the annealing temperature after illumination with IR light at 20 K. The Si concentration is 5×10^{18} cm^{-3} in both layers (samples 10 and 11). The core annihilation parameter was measured in the dark at 20 K. The closed symbols and the arrows indicate the core annihilation parameter after cooling the sample from 295 K and the effect of illumination, respectively. The solid lines are guides to the eye.

The removal of the vacancy signal and its recovery are correlated to the photo-Hall experiments (Fig. 3). The quenching of the vacancy signal appears in the layers $x=0.36$ and 0.51, in which the persistent photoconductivity effect was observed, but not in $Ga_{0.51}In_{0.49}P$. Moreover, the vacancy signal recovers at the same temperature range from 60 to 140 K at which the persistent photoconductivity disappears. The disappearance of the vacancy signal after exposure to IR light as well as in thermal equilibrium above 350 K was earlier observed in Si-doped $Al_xGa_{1-x}As$.[18,19]

IV. Si IN $Al_xGa_{0.51-x}In_{0.49}P$: DEEP DONOR LEVELS AND THE LOCAL STRUCTURE OF THE *DX* CENTER

The appearance of a deep ground state of the Si donor and the persistent photoconductivity effect suggest that *DX* centers are formed in $Al_xGa_{0.51-x}In_{0.49}P$. Below we will demonstrate that the appearance of the *DX* level into the band gap around $x\approx0.1$ gives a consistent picture of the experimental findings. $Al_xGa_{0.51-x}In_{0.49}P$ is found to be very similar to the $Al_xGa_{1-x}As$ system. We will give evidence for identifying the vacancylike defect as the *DX* center, and discuss its local structure.

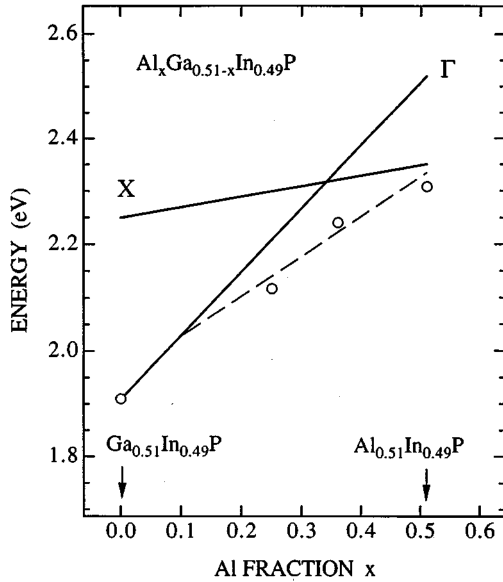

FIG. 7. The thermal binding energies of the dominant donor levels at different alloy compositions from $x=0$ ($Ga_{0.51}In_{0.49}P$) to $x=0.51$ ($Al_{0.51}In_{0.49}P$). The binding energies were taken from the slopes of the $\ln(n_{\mathrm{Hall}})$-vs-T^{-1} curves in Fig. 2. The positions of the Γ and X minima of the conduction band with respect to the valence-band edge at $T=300$ K are from Refs. 10, 43, and 44.

A. Donor levels

The Arrhenius plot $\ln(n_{\mathrm{Hall}})$-vs-T^{-1} from 130 to 300 K shows the carrier freeze-out into a deep electron level (Figs. 2 and 3). The free-electron density is thermally activated, and we can assume that in this temperature range the occupation of the deep level is in equilibrium with the electron states in the conduction band.

From total-energy calculations, a metastable donor configuration is found for a negatively charged donor.[13] The donor impurity then behaves as a negative-U center capturing *two* electrons. In that case the electron density in the conduction band (n) of a nondegenerate semiconductor with N_D donors compensated by N_A acceptors is given by[31,42]

$$\frac{n^2(N_D+N_A+n)}{N_D-N_A-n}=N_C^2\exp\left[-\frac{2E_D}{k_BT}\right]. \tag{2}$$

In Eq. (2), N_C is the effective density of states in the conduction band, and E_D is the energy for a transfer of an electron from the deep donor level to the lowest-lying band edge. The electronic degeneracy factor is included in the entropy term of the thermal activation energy, and the contribution from the excited (shallow) states of the donor is neglected. When $n \ll N_A < N_D$, i.e., when the donors are strongly compensated, the slope of the $\ln(n_{\mathrm{Hall}})$-vs-T^{-1} curve will determine the thermal ionization enthalpy H_D of the deep donor. This condition should be true at low temperatures, because there are many more ionized donors to capture electrons than there are free electrons in the conduction band.

Figure 7 shows the relative positions of the Γ and X minima of the conduction band in $Al_xGa_{0.51-x}In_{0.49}P$ from $x=0$ to 0.51.[10,43,44] The thermal activation energies taken from the slopes of the $\ln(n_{\mathrm{Hall}})$-vs-T^{-1} curves in Fig. 2 are plotted in the same figure. As indicated above, the apparent activation energy yields the thermal ionization energy of the deep donor level. This is expected to be valid even if the ground state of the donor were neutral.[45] However, appreciable differences between the true electron concentration n and the Hall carrier concentration n_{Hall} may appear at the crossover from the direct to indirect band gap at $x\approx 0.33$ because of the distribution of electrons between the different conduction-band minima. From Fig. 7, the temperature variation of n/n_{Hall} can only effect the experimental activation energy in the layer $x=0.36$ which is close to the crossover point.[46] At the other alloy composition the electrons predominantly occupy either the Γ or X conduction-band minimum.

The variation of the position of the deep donor level with the alloy composition can be estimated from Fig. 7. For $x \geqslant 0.25$ the present experimental data can be approximately described by a linear variation of the energy level with alloying (in eV) $\Delta E \cong 0.72\Delta x$ with respect to the edge of the valence band. The variation of the Γ band edge measured from the valence-band maximum is given by $E_\Gamma = 1.91+1.22x$.[43] The thermal binding energy relative to the conduction-band minimum for $x \leqslant 0.33$ therefore varies with the alloy composition as $\Delta E_D \cong 0.50\Delta x$, and it is approximately given by $E_D=(0.50x-0.05)$ eV.

The thermal binding energy estimated above would imply that the deep donor level appears in the band gap around $x\approx 0.1$. Rapid increase of the Se-related deep levels in Se-doped $Al_xGa_{0.51-x}In_{0.49}P$ has been reported at the same alloy composition.[12]

The variation of the position of the deep donor level with the alloy composition is very similar to that of the *DX* center in $Al_xGa_{1-x}As$.[46] Chadi and Chang[13] suggested a simple expression for the alloy composition dependence of the *DX* binding energy. As the *DX* center is a localized defect, the variation of its energy level relative to the valence-band maximum should be nearly equal to the change of the average energy of the lowest conduction band. They indicated that the average energy of the conduction band closely follows the L minimum of the conduction band, and that this should hold for many III-V alloys. The poorly known band structure and in particular the L minimum of the conduction band make a direct comparison between the deep donor level and the conduction band in $Al_xGa_{0.51-x}In_{0.49}P$ difficult. The variation of the position of the deep donor level $\Delta E \cong 0.72\Delta x$ compared to the valence-band edge is, however, very similar to variation of the L minimum of the conduction band in other alloys of Al and Ga. In $Al_xGa_{1-x}As$ the variation of the indirect band gap $\Delta E_L = 0.75\Delta x$ has been estimated.[45] The indirect band gap from the Γ point to the L minimum of the conduction band increases by $\Delta E_L = 0.78$ eV from GaP to AlP, and 0.72 eV from GaSb to AlSb.[47]

In conclusion, we observe a rather deep donor level in $Al_xGa_{0.51-x}In_{0.49}P$. It appears into the band gap as the ground state of the donor when the bottom of the conduction band is shifted to higher energies due to Al alloying. With respect to the valence and conduction bands the deep donor level varies with the alloy composition in a very similar way as the *DX* center in $Al_xGa_{1-x}As$.

B. Persistent photoconductivity: Identification of the vacancy defects

Illumination of n-type Si-doped $Al_xGa_{0.51-x}In_{0.49}P$ with IR or red light at low temperatures persistently increases the concentration of electrons in the conduction band (Fig. 3). The persistent photoconductivity effect and the variation of the thermal binding energy of the dominant donor state with the alloy composition give an indication of the existence of DX centers.

Persistent photoconductivity was demonstrated in Si-doped $Al_xGa_{0.51-x}In_{0.49}P$ with $x=0.36$, and in $Al_{0.51}In_{0.49}P$. At both alloy compositions the conduction band is indirect (Fig. 7). In the layer $x=0.36$, the number of electrons in the conduction band increases by one order of magnitude after illumination. The electron concentration at 70 K is, however, only 10% of the number of Si atoms 5×10^{18} cm^{-3} in the layer. It is equivalent to the persistent photoconductivity effect in $Al_xGa_{1-x}As$ with an indirect band gap.[30,31] The shallow donor level associated with the X minimum in $Al_xGa_{1-x}As$ has a rather high binding energy. Electrons therefore partly occupy the shallow donor levels, and the number of electrons in the conduction band remain much smaller than the donor concentration. We anticipate that the rather low free-electron concentration in $Al_xGa_{0.51-x}In_{0.49}P$ after illumination is due to the same effect, i.e., the distribution of electrons between the conduction-band states and the hydrogenic donor levels associated with the X minimum below 70 K.

Carrier separation due to macroscopic potential barriers between low and high resistivity regions of inhomogeneous material may also give rise to persistent photoconductivity effects at low temperatures.[48] It is usually difficult to distinguish between the different possible origins by the measurement of the photoconductivity. In MBE-grown ternary and quaternary alloys some variation of the composition may occur depending on the growth conditions. Observation of deep donor levels in the layers in which the persistent photoconductivity appears suggests that it can be associated with the DX centers. This is further supported by the earlier observations of deep electron levels related to donor impurities showing persistent photoeffects in $Al_xGa_{0.51-x}In_{0.49}P$ grown by different techniques. Such centers have been reported in MBE-grown Si-doped,[11] metal-organic vapor-phase-epitaxy-grown Se-doped,[12] and vapor-phase-epitaxy-grown S-doped layers.[49]

The vacancy signal which dominates positron annihilation in Si-doped $Al_xGa_{0.51-x}In_{0.49}P$ from 20 to 450 K disappears after illumination with IR light. Below 60 K the phenomenon is persistent, and the vacancy can only be seen if temperature is raised. This vacancy defect shows a similar correlation to Si doping and the alloy composition as the DX center. It only appears in n-type Si-doped layers, and it cannot be observed in $Ga_{0.51}In_{0.49}P$ in which the donor level is shallow.

Phenomenological comparisons between the characteristics of positron annihilation at the DX center in $Al_xGa_{1-x}As$ (Refs. 18 and 19) and the evidence presented here clearly support the assertion that the defect state in Si-doped $Al_xGa_{0.51-x}In_{0.49}P$ is due to the Si-DX center. Optical ionization converts the DX center into a shallow hydrogenic donor. In Si- and Te-doped $Al_xGa_{1-x}As$ the optical ionization cross section of the DX center is equal to the ionization cross section of the vacancy. The variation of the energy barrier for electron capture at the DX center with the donor species and the alloy composition gives a good description of the recovery of the vacancy signal after illumination.[18,19] In analogy with $Al_xGa_{1-x}As$, the persistent disappearance of the vacancy signal after illumination, and the reappearance of the vacancy when the persistent photoconductivity decays between 60 and 120 K (Figs. 3 and 6) in Si-doped $Al_xGa_{0.51-x}In_{0.49}P$ are correlated to the DX center. The recovery after illumination occurs at a markedly broader temperature range in a quaternary alloy $Al_xGa_{0.51-x}In_{0.49}P$ than in $Al_xGa_{1-x}As$. This may be due to a variation of the local environment of the donors giving rise to a distribution of capture energies for electrons. Previously very broad deep-level transient spectroscopy (DLTS) spectra from the Si DX center in $Al_xGa_{0.51-x}In_{0.49}P$ has been reported.[11]

Thermal ionization of the DX center gives further insight into the origin of the vacancy defect. In $Al_xGa_{1-x}As$ the disappearance of the vacancy signal above 350 K was associated with the ionization of the Si-DX center in thermal equilibrium.[19] The data yields thermal ionization energy in good agreement with the values based on Hall experiments. The Hall carrier concentration in Si-doped $Al_xGa_{0.51-x}In_{0.49}P$ implies that of the order of 10^{18} cm^{-3} DX centers are occupied at room temperature. The thermal ionization of those centers can explain the disappearance of the vacancy signal between 450 and 700 K.

Based on the detailed study of the Si-DX center in $Al_xGa_{1-x}As$, and the properties of the vacancy defects in $Al_xGa_{0.51-x}In_{0.49}P$, we come to the conclusion that the defect which dominates positron annihilation in Si-doped $Al_xGa_{0.51-x}In_{0.49}P$ is the DX center. All the experimental results point out that the DX center traps a positron when the deep level is occupied, but trapping disappears when the DX center is optically or thermally ionized.

C. Local structure of the DX center

We now turn to the local structure of the DX center. Positron annihilation demonstrates that the Si-DX center in $Al_xGa_{0.51-x}In_{0.49}P$ has a vacancylike structure. This was found earlier from the Doppler experiments in Si- and Te-doped $Al_xGa_{1-x}As$,[18,50] as well as from positron lifetime measurements in Te-doped $Al_xGa_{1-x}Sb$.[51]

The metastable configuration of the DX center reached by optical ionization no longer acts as a positron trap. A transition into a positive charge state would make the vacancy unobservable. Directly from the positron experiment we can only conclude that either the vacancy disappears or that it becomes positively charged. However, in $Al_xGa_{1-x}As$ it has been shown that the DX levels and the hydrogenic levels originate from the same impurity atom,[52] and in the metastable configuration of the DX center the hydrogenic states of an isolated substitutional donor impurity have been seen by infrared absorption,[53] Hall measurements,[54] and electron paramagnetic resonance.[55,56] Assuming the same basic structure of the DX center, the Si atom would be at the substitutional site of the group-III atom (Ga, In, Al) after optical ionization of the Si DX center in $Al_xGa_{0.51-x}In_{0.49}P$ as well. To reconcile the vacancylike structure of the DX center with

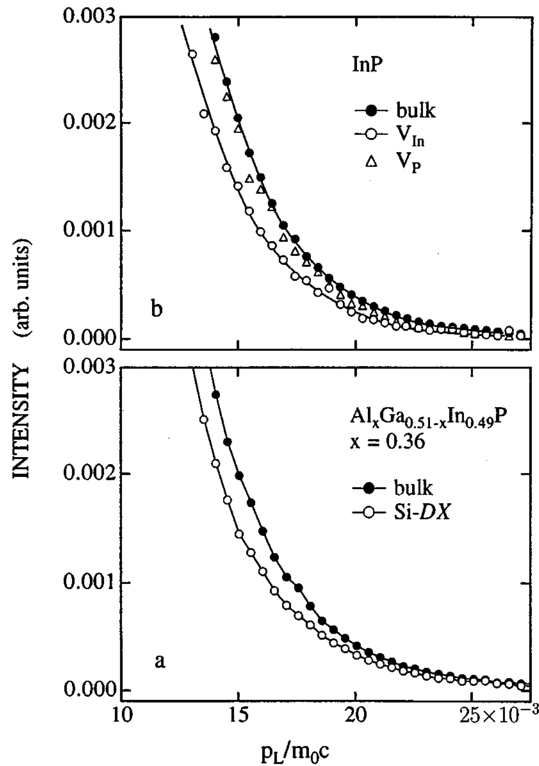

FIG. 8. (a) The core annihilation spectra in undoped and Si-doped $Al_xGa_{0.51-x}In_{0.49}P$ with $x=0.36$ and the Si concentration is 5×10^{18} cm^{-3} (sample 10) measured using the coincidence detection of the two annihilation γ rays. (b) The core annihilation spectra for bulk InP, and In- and P- vacancies in InP. Data are from Ref. 28. The solid lines are guides to the eye.

these results requires a large relaxation of atoms from the substitutional geometry when electrons are captured at the *DX* level.

The valence annihilation parameter for the Si-*DX* center in $Al_xGa_{0.51-x}In_{0.49}P$ with $x=0.36$ is $S_{DX}/S_B=1.015-1.02$. It is smaller than the valence annihilation parameter for Ga or As vacancies in GaAs.[40,41] It is also smaller than the valence annihilation parameter for either the In or P vacancy in InP. We can therefore assume that the vacancy associated with the *DX* center is somewhat smaller than an isolated vacancy. A similar conclusion was found in the case of *DX* centers in $Al_xGa_{1-x}As$ (Refs. 18 and 19) and $Al_xGa_{1-x}Sb$,[51] as well as in the case of the *EL*2 defect in GaAs.[57]

To study the chemical nature and the lattice site of the *DX* center further, the core electron annihilation spectra were measured using the coincidence technique to reduce the background.[28] Thereby the momentum distribution of the annihilating core electrons can be studied. The spectra for undoped and Si-doped $Al_xGa_{0.51-x}In_{0.49}P$ with $x=0.36$ are plotted in Fig. 8 from $\Delta E_\gamma=3.3$–7.0 keV. It corresponds to annihilations with a longitudinal momentum component p_L from 13×10^{-3} to $27\times10^{-3} m_0c$. To compare the Si-*DX* center with vacancy defects in InP, we calculate the core annihilation parameter W using the same window $15\times10^{-3}\leqslant p_L/m_0c\leqslant 20\times10^{-3}$, corresponding to 15–20 mrad in a one-dimensional angular correlation measurement as in Ref. 28. For the Si-*DX* center in $Al_xGa_{0.51-x}In_{0.49}P$ with $x=0.36$, it yields $W_{DX}/W_B=0.75$.

The core annihilation parameter $W_{DX}/W_B=0.75$ for the Si-*DX* centers in $Al_xGa_{0.51-x}In_{0.49}P$ ($x=0.36$) is markedly smaller than in $Al_xGa_{1-x}As$, where $W_{DX}/W_B=0.86$.[58] Two possible mechanisms can explain the difference. First, the distortions around the donor impurities can be different. There is, however, another possibility. Considering the core electron annihilation, a major difference between these two materials is the very different core shells of the group-V atoms P and As. The core annihilation parameter can also change if the atomic configurations are equivalent but the nearest-neighbor atoms—that is, P or As—around the vacancy are different.

The core annihilation parameters have been used to identify the P and In vacancies V_P and V_{In} in InP.[28] The magnitude of the core electron annihilation is much smaller in the In vacancy than in the P vacancy. The neighboring P atoms of an In vacancy give a negligible core electron annihilation signal. In a P vacancy V_P the annihilation with the electrons of the In core shells yields almost as strong a core annihilation component as in the bulk. In Ref. 28 the core annihilation parameters $W_{V_{In}}/W_B=0.70$ and $W_{V_P}/W_B=0.94$ were calculated using the window $(15–20)\times10^{-3} m_0c$. The core annihilation parameter for the Si-*DX* center in $Al_xGa_{0.51-x}In_{0.49}P$, $W_{DX}/W_B=0.75$, is similar to that found for V_{In} in InP but much lower than the core annihilation parameter for V_P. We therefore come to the conclusion that the vacancy in the Si-*DX* center has P atoms as its nearest neighbors, in analogy with the In vacancy, i.e., the vacancy must be in the group-III sublattice.

Finally, we compare the local structure of the *DX* center with the theoretical models. It has become increasingly evident that the vacancy-interstitial model accounts for the electrical and optical properties of the *DX* center in $Al_xGa_{1-x}As$.[14] Donors can take two different configurations. One is the simple substitutional geometry which gives rise to the effective-mass states. The other is characterized by a large displacement of the column-IV donor atom along the $\langle 111\rangle$ direction. The distorted geometry of the donor impurity can be viewed as a vacancy-interstitial pair. This is in agreement with the structural data from the positron annihilation experiments which directly indicate the vacancylike structure of the *DX* center. The impurity atom at an interstitial site next to the vacancy could also account for the fact that the vacancy in the *DX* center is smaller in size than an isolated vacancy.[18,51] The very different structures of the core shells of the group-III atoms (Ga,In) and the group-V atom (P) in $Al_xGa_{0.51-x}In_{0.49}P$ suggest a direct identification of the vacancy. To explain the core electron annihilation in the Si-*DX* center, we must assume that the vacancy has P atoms as its nearest neighbors. This is in agreement with the displacement of the Si atom off the substitutional (Al, Ga, In) lattice site. Such an identification was not possible in $Al_xGa_{1-x}As$ because of the rather similar structures of Ga and As core shells.

V. CONCLUSION

We have investigated the donor levels and the local structure of the *DX* center in Si-doped $Al_xGa_{0.51-x}In_{0.49}P$ grown

by gas-source molecular-beam epitaxy and lattice matched to GaAs. The experimental techniques include Hall and SIMS measurements and positron spectroscopy.

Compensation of free carriers, thermal binding energy of the dominant donor level, and the concentration of vacancy-like defects in the n-type layers depend strongly on the alloy composition. In the ternary alloy $Ga_{0.51-x}In_{0.49}P$, the Si donors form only shallow donor states. Compensation of electrons remains rather small even at very high donor concentrations up to 3×10^{19} cm^{-3}. In quaternary alloys with $x\geqslant0.25$ a deep electron trapping center was observed. Trapping of electrons at the deep level limits the concentration of mobile electrons at $(1–2)\times10^{18}$ cm^{-3}. Hall measurements revealed an activated behavior of the mobile electron concentration. The thermal binding energy is $\sim$0.1 eV, when $x=0.25$. After illumination with IR or red light, the persistent photoconductivity effect is observed at $T\leqslant120$ K. The appearance of the DX level into the band gap above $x\approx0.1$ gives a consistent picture of the experimental findings. $Al_xGa_{0.51-x}In_{0.49}P$ appears very similar to the $Al_xGa_{1-x}As$ system.

The vacancy-type defect, which is correlated to the deep electron center, was identified as the Si-DX center. The local structure of the Si-DX center from positron annihilation spectroscopy is equivalent to that found earlier in $Al_xGa_{1-x}As$. In particular, we find that, when the DX level is filled, the Si-DX center is a vacancylike defect. The very different core shell structures of the cation site (Ga,In) and the anion site (P) atoms suggest a direct identification of the vacancy sublattice. We find direct evidence that the vacancy has P atoms as its nearest neighbors, and identify it as a vacancy in the (Al, Ga, In) sublattice. The structural data give support to the vacancy-interstitial model which predicts that the donor impurities can take two different configurations in sp-bonded semiconductors.

ACKNOWLEDGMENTS

We would like to thank A. Fontell in Accelerator Laboratory in University of Helsinki for providing the ion implanted reference samples for SIMS experiments. This work has been supported by the Academy of Finland (EPIMATTER project).

---

[*]Present address: VTT Building Technology, Fire Technology, P. O. Box 1803, 02044 VTT, Finland.

[1] S. S. Ou, J. J. Yang, and C. J. Hwang, Appl. Phys. Lett. **61**, 892 (1992).
[2] G. Hatagoshi, K. Nitta, K. Itaya, Y. Nishikawa, M. Ishikawa, and M. Okajima, Jpn. J. Appl. Phys. **31**, 501 (1992).
[3] P. M. Mooney, J. Appl. Phys. **67**, R1 (1990).
[4] *Physics of DX Centers in GaAs Alloys*, edited by J. C. Bourgoin (Sci-Tech, Lake Isabella, CA, 1990).
[5] D. V. Lang and R. A. Logan, Phys. Rev. Lett. **39**, 635 (1977).
[6] D. V. Lang, R. A. Logan, and M. J. Jaros, Phys. Rev. B **19**, 1015 (1979).
[7] M. I. Nathan, P. M. Mooney, P. M. Solomon, and S. L. Wright, Appl. Phys. Lett. **47**, 628 (1985).
[8] M. I. Nathan, P. M. Mooney, P. M. Solomon, and S. L. Wright, Surf. Sci. **174**, 431 (1986).
[9] K. R. Hoffman and E. Kohn, Electron. Lett. **22**, 335 (1986).
[10] H. Asahi, Y. Kawamura, and H. Nagai, J. Appl. Phys. **53**, 4928 (1982).
[11] S. Nojima, H. Tanaka, and H. Asahi, J. Appl. Phys. **59**, 3489 (1986).
[12] Miyoka O. Watanabe and Yasuo Ohba, J. Appl. Phys. **60**, 1032 (1986).
[13] D. J. Chadi and K. J. Chang, Phys. Rev. Lett. **61**, 873 (1988).
[14] J. Dabrowski and M. Scheffler, in *Defects in Semiconductors*, edited by G. Davies, G. L. DeLeo, and M. Stavola, Material Science Forum Vols. 83-87 (Trans Tech, Zürich, 1992), p. 735.
[15] J. Dabrowski and M. Scheffler, Phys. Rev. Lett. **60**, 2183 (1988).
[16] D. J. Chadi and K. J. Chang, Phys. Rev. Lett. **60**, 2187 (1988).
[17] D. J. Chadi, Phys. Rev. Lett. **72**, 534 (1994).
[18] J. Mäkinen, T. Laine, K. Saarinen, P. Hautojärvi, C. Corbel, V. M. Airaksinen, and P. Gibart, Phys. Rev. Lett. **71**, 3154 (1993).
[19] J. Mäkinen, T. Laine, K. Saarinen, P. Hautojärvi, C. Corbel, V. M. Airaksinen, and J. Nagle, Phys. Rev. B **52**, 4870 (1995).
[20] H. Asonen, K Rokennnus, K. Tappura, M. Hovinen, and M. Pessa, J. Cryst. Growth **105**, 101 (1990).
[21] A. R. Bayly, M. Cummings, P. Vohralik, K. Williams, D. R. Kingham, A. R. Waugh, and J. M. Walls, in *SIMS VI*, edited by A. Benninghoven *et al.* (Wiley, Chichester, 1988), pp. 169–172.
[22] R. G. Wilson, F. A. Stevie, and C. W. Magee, *Secondary Ion Mass Spectrometry: A Practical Handbook for Depth Profiling* (Wiley, New York, 1989).
[23] *Positrons in Solids*, edited by P. Hautojärvi, Topics in Current Physics Vol. 12 (Springer-Verlag, Heidelberg, 1979).
[24] *Positron Solid State Physics*, edited by W. Brandt and A. Dupasquier (North-Holland, Amsterdam, 1983).
[25] P. J. Schultz and K. G. Lynn, Rev. Mod. Phys. **60**, 701 (1988).
[26] K. G. Lynn, J. R. MacDonald, R. A. Boie, L. C. Feldman, J. D. Gabbe, M. F. Robbins, E. Bonderup, and J. Golovchenko, Phys. Rev. Lett. **38**, 241 (1977).
[27] K. G. Lynn, J. E. Dickman, W. L. Brown, M. F. Robbins, and E. Bonderup, Phys. Rev. B **20**, 3566 (1979).
[28] M. Alatalo, H. Kauppinen, K. Saarinen, M. J. Puska, J. Mäkinen, P. Hautojärvi, and R. M. Nieminen, Phys. Rev. B **51**, 4176 (1995).
[29] M. Suzuki, M. Ishikawa, K. Itaya, Y. Nishikawa, G. Hatakoshi, Y. Kokubun, J. Nishizawa, and Y. Oyama, J. Cryst. Growth **115**, 498 (1991).
[30] M. Mizuta and K. Mori, Phys. Rev. B **37**, 1043 (1988).
[31] J. E. Dmochowski, L. Dobaczewski, J. M. Langer, and W. Jantsch, Phys. Rev. B **40**, 9671 (1989).
[32] R. N. West, in *Positrons in Solids* (Ref. 23), p. 89.
[33] R. Krause-Rehberg, A. Polity, W. Siegel, and G. Kühnel, Semicond. Sci. Techol. **8**, 290 (1993).
[34] J. Mäkinen, C. Corbel, P. Hautojärvi, P. Moser, and F. Pierre, Phys. Rev. B **39**, 10 162 (1989).
[35] J. Mäkinen, P. Hautojärvi, and C. Corbel, J. Phys. Condens. Matter **3**, 7217 (1991).
[36] R. Krause, A. Klimakow, F. M. Kiesling, A. Polity, P. Gille, and M. Schenk, J. Cryst. Growth **101**, 512 (1990).
[37] M. J. Puska, C. Corbel, and R. M. Nieminen, Phys. Rev. B **41**, 9980 (1990).
[38] M. J. Stott and R. N. West, J. Phys. F **8**, 635 (1978).
[39] K. Saarinen, P. Hautojärvi, A. Vehanen, R. Krause, and G.

Dlubek, Phys. Rev. B **39**, 5287 (1989).

[40] K. Saarinen, P. Hautojärvi, P. Lanki, and C. Corbel, Phys. Rev. B **44**, 10 585 (1991).

[41] R. Ambigapathy, A. A. Manuel, P. Hautojärvi, K. Saarinen, and C. Corbel, Phys. Rev. B **50**, 2188 (1994).

[42] K. Khachaturyan, E. R. Weber, and M. Kaminska, in Proceedings of the 15th International Conference on Defects in Semiconductors [Mater. Sci. Forum **38-41**, 1067 (1989)].

[43] C. Nozaki, Y. Ohba, H. Sugawara, S. Yasuami, and T. Nakasini, J. Cryst. Growth **93**, 406 (1988).

[44] A. Onton, M. R. Lorentz, and W. Reuter, J. Appl. Phys. **43**, 3420 (1971).

[45] T. N. Theis, P. M. Mooney, and B. D. Parker, J. Electron. Mater. **20**, 35 (1991).

[46] N. Chand, T. Henderson, J. Klem, W. T. Masselink, R. Fischer, Y. Chang, and H. Morkoç, Phys. Rev. B **30**, 4481 (1984).

[47] *Semiconductors: Group IV Elements and III-V Compounds, Data in Science and Technology*, edited by R. Poerschke and O. Madelung (Springer-Verlag, Berlin, 1991).

[48] H. J. Queisser and D. E. Theodorou, Phys. Rev. Lett. **43**, 401 (1979).

[49] K. Kitahara, M. Hoshino, K. Kodama, and M. Ozeki, Jpn. J. Appl. Phys. **25**, L534 (1986).

[50] T. Laine *et al.*, Phys. Rev. B (to be published).

[51] R. Krause-Rehberg, Th. Drost, A. Polity, G. Roos, G. Pensl, D. Volm, B. K. Meyer, G. Bischopink, and K. W. Benz, Phys. Rev. B **48**, 11 723 (1993).

[52] T. N. Theis, T. F. Keuch, L. Palmateer, and P. M. Mooney, in *Gallium Arsenide and Related Compounds*, edited by B. de Cremoux, IOP Conf. Proc. No. 74 (Institute of Physics and Physical Society, Bristol, 1984).

[53] J. E. Dmochowski, J. E. Dobaczewski, L. Dobaczewski, J. M. Langer, and W. Jantsch, Phys. Rev. B **40**, 9671 (1989).

[54] M. Mizuta and K. Mori, Phys. Rev. B **37**, 1043 (1988).

[55] P. M. Mooney, W. Wilkening, U. Kaufmann, and T. F. Kuech, Phys. Rev. B **39**, 5554 (1989).

[56] H. J. von Bardeleben, J. C. Bourgoin, P. Basmasji, and P. Gibart, Phys. Rev. B **40**, 5892 (1989).

[57] K. Saarinen, S. Kuisma, P. Hautojärvi, C. Corbel, and C. LeBerre, Phys. Rev. B **49**, 8005 (1994).

[58] Note that this value is different from the value 0.936 given in Ref. 18 because of the different energy window used to calculate the core annihilation parameter.